Electronic Supplementary Information (ESI)

for

Lighting up endogenous H_2O_2 in tumor microenvironment using dual-mode nanoprobe by long afterglow and MR bioimaging

Yiming Wang[a], Jintao He[a], Rong Feng[a], Jingwen Chen[a], Gege Xie[a], Shengrong Yu*[ab], Yong-Xiang Wu*[ab], and Keqi Tang*[ab]

[a.] Institute of Mass Spectrometry, Zhejiang Engineering Research Center of Advanced Mass spectrometry and Clinical Application, School of Material Science and Chemical Engineering, Ningbo University, Ningbo 315211, China.

[b.] Zhenhai Institute of Mass Spectrometry, Ningbo 315211, China.

* To whom correspondence should be addressed.

E-mail: yushengrong@nbu.edu.cn

wuyongxiang@nbu.edu.cn

tangkeqi@nbu.edu.cn

Table of contents

1. Reagents and Materials

Gallium oxide (Ga_2O_3), chromic nitrate nonahydrate ($Cr(NO_3)_3 \cdot 9H_2O$), zinc nitrate hexahydrate ($Zn(NO_3)_2 \cdot 6H_2O$), potassium permanganate ($KMnO_4$) was purchased from Aladdin (Shanghai, China). 2-Morpholinoethanesulphonic acid (MES) was purchased from Shanghai Sangon Biological Engineering Technology & Services (Shanghai, China). H_2O_2 stimulant Phorbol 12-myristate 13-acetate (PMA) and H_2O_2 scavenger N-acetyl-L-cysteine (NAC) were purchased from Beyotime Biotechnology (Shanghai, China). All other reagents were of analytical grade (Aladdin, Shanghai China) and used without further purification.

2. Apparatus

High-resolution transmission electron microscope (HRTEM, JEM-2100F, 200kV) was employed for the morphological characterization of the nanomaterials. RF-6000 fluorescence spectrophotometer (Shimadzu, Japan) was obtained for fluorescence spectrograms. The fluorescence microscopy images of cell were recorded by a Confocal Fluorescence Microscope (Olympus Fluoview FV3000, Japan). The measuring of longitudinal relaxation time (T_1) was obtained by Bruke PharmaScan70/16US analyzing and imaging system (Institute of Basic Medicine and Cancer, Chinese Academy of Sciences, Hangzhou, China).

3. Specificity Investigations

Mix ZGC with different solutions of various that ions including the common metal cations (K^+, Na^+, Mg^{2+}, Mn^{2+}, Zn^{2+}, Fe^{3+}), common anions (Cl^-, NO^{3-}, SO_4^{2-}, HCO_3^-), Glu and H_2O_2. The mixture was maintained at 25 °C for 30 min to facilitate the reaction. Fluorescence emission spectra ranging from 650 nm to 730 nm were obtained using an excitation wavelength of 488 nm. All fluorescence measurements were conducted in triplicate.

4. Supplementary Figures and Tables

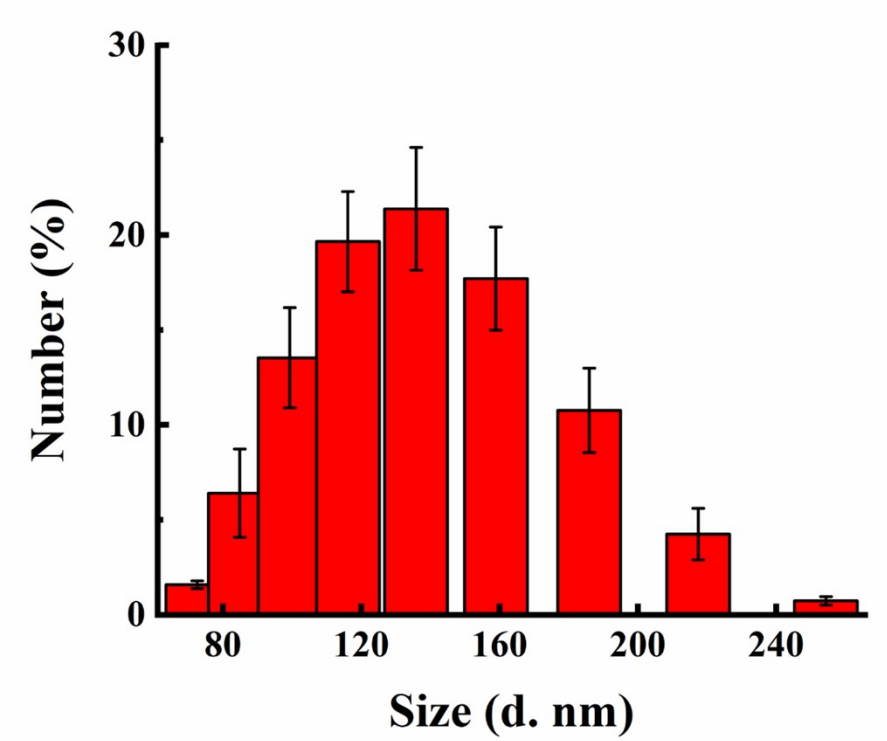

Figure S1. The particle size distribution of ZGC was determined based on dynamic light scattering.

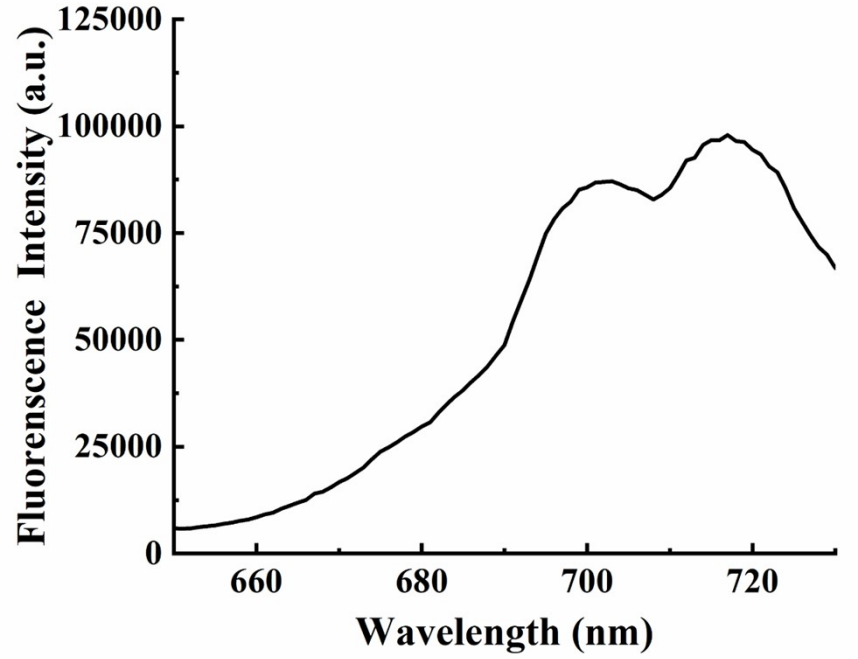

Figure S2. The luminescence spectrum of ZGC nanoparticles (290.0 μg/mL) in deionized H_2O.

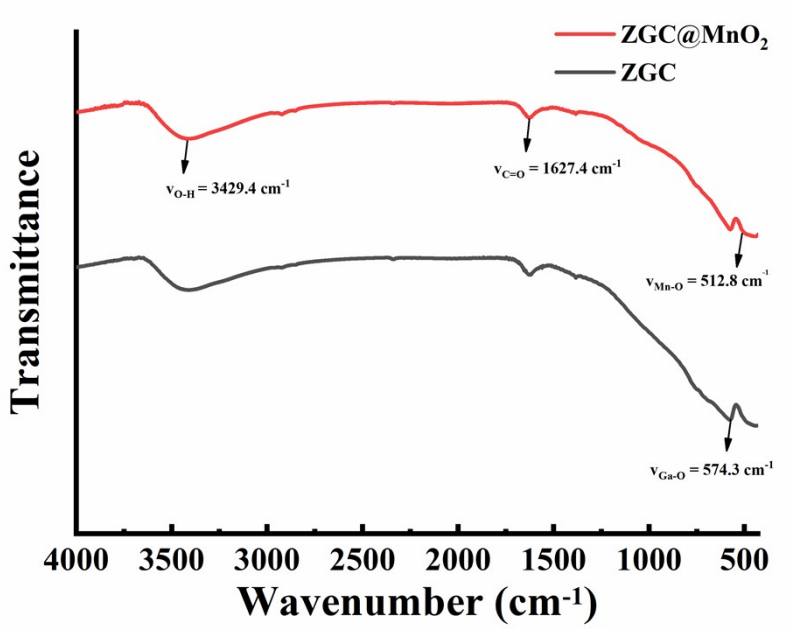

Figure S3. Fourier transform infrared spectrometer (FT-IR) spectrogram of ZGC and ZGC@MnO_2.

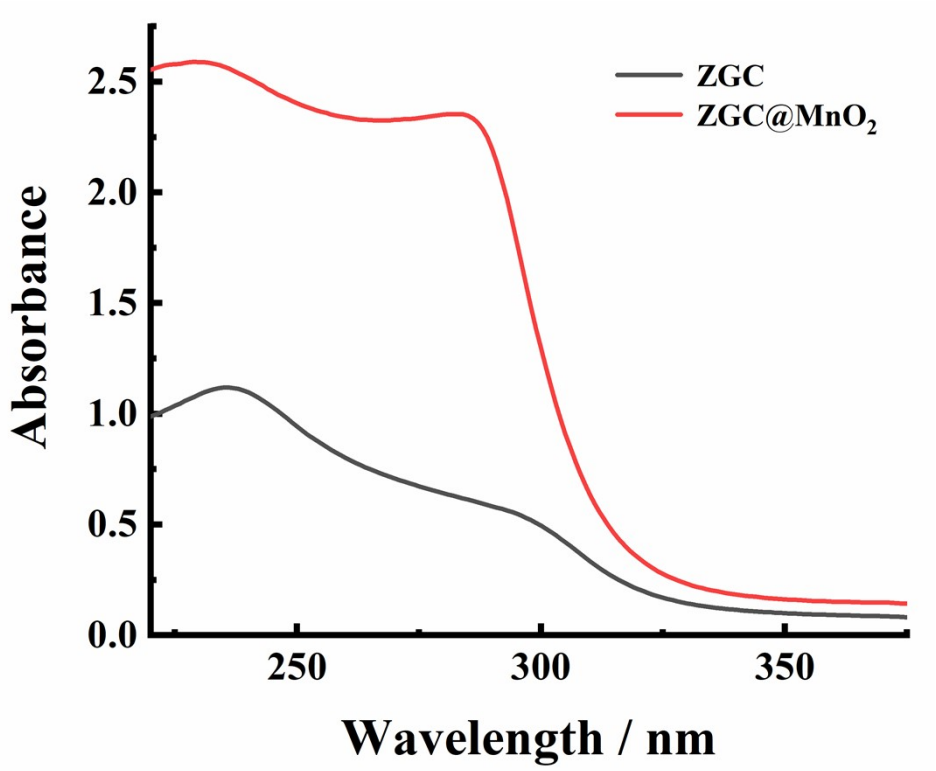

Figure S4. UV−vis absorption spectra of ZGC and ZGC@MnO_2 (290.0 μg/mL) in PBS (pH = 5.0, 100 mM).

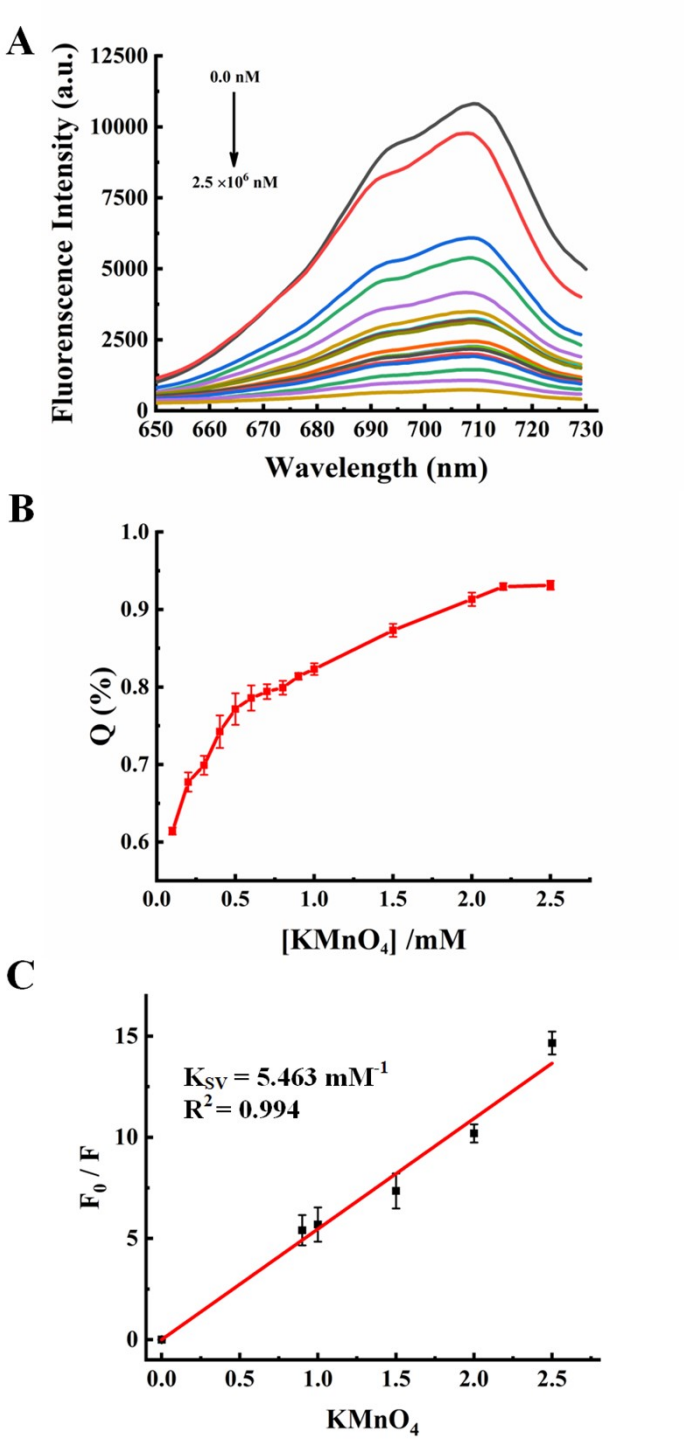

Figure S5. (A) Fluorescence quenching experiment of ZGC (75 μg/mL) under different concentrations of $KMnO_4$ (0 nM; 1 nM; 10 nM; 20 nM; 25 nM; 0.1 mM; 0.2 mM; 0.3 mM; 0.4 mM; 0.5 mM; 0.6 mM; 0.7mM; 0.8 mM; 0.9 mM; 1.0 mM; 1.5mM; 2.0mM; 2.5 mM). (B) Fluorescence quenching rate (Q) versus different concentrations of $KMnO_4$. (C) Stern−Volmer quenching graph of $KMnO_4$ in the existence of ZGC. The range of quenching efficiency of MnO_2 nanosheets was evaluated via the Stern-Volmer equation: $\frac{F_0}{F} = 1 + K_{sv}[Q]$.

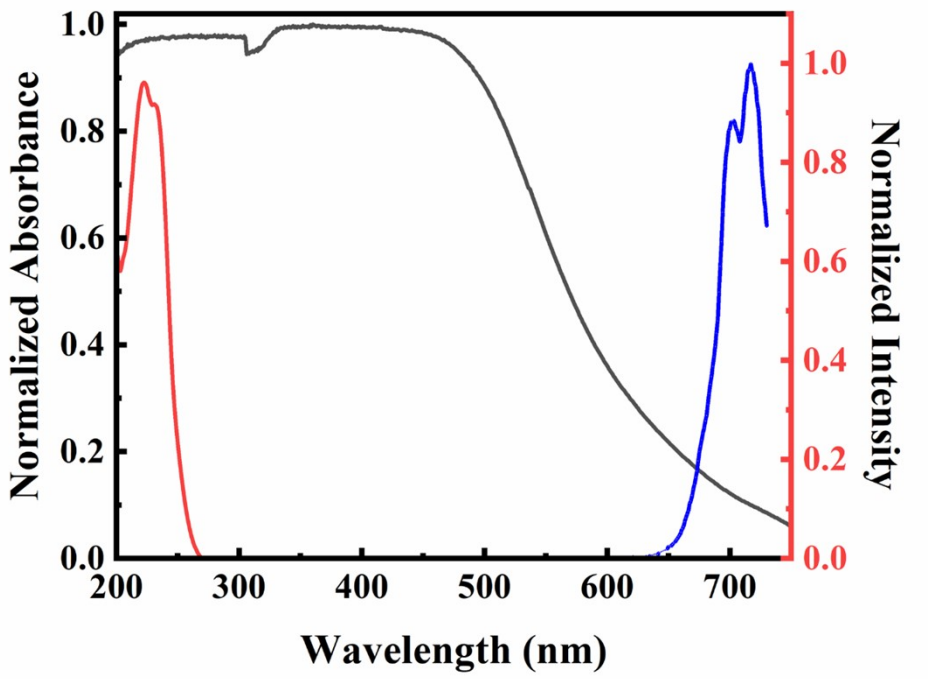

Figure S6. The UV-vis absorption spectrogram of MnO_2 nanosheets (grey line), the fluorescence spectrogram of prepared ZGC: the excitation (red line) and emission (blue line).

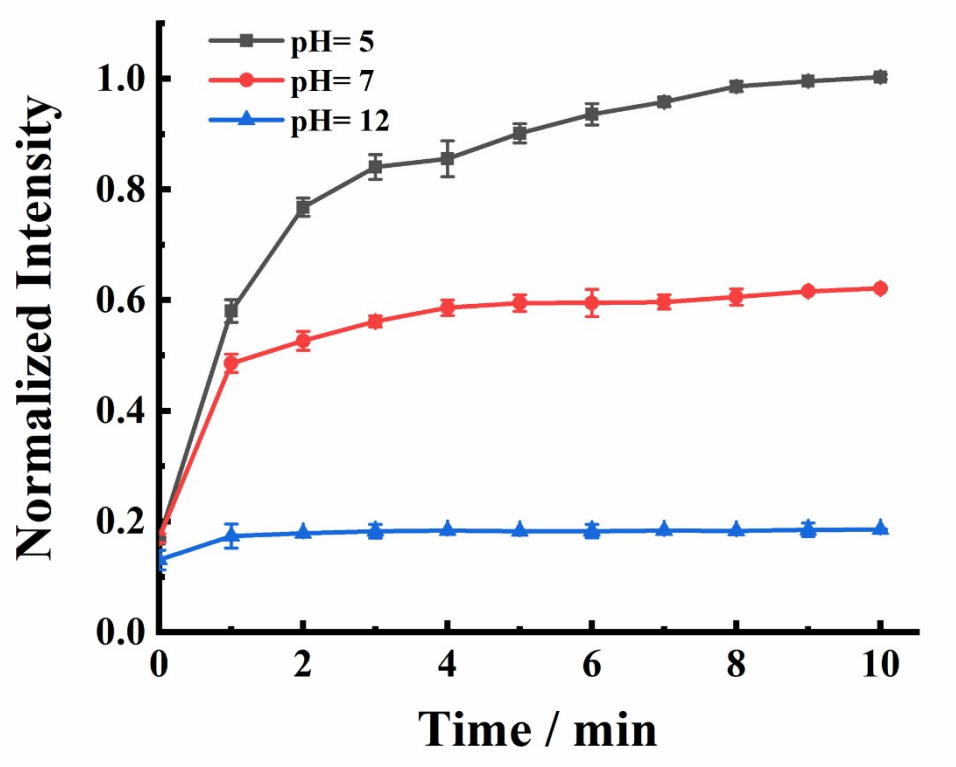

Figure S7. Fluorescence recovery time curve of ZGC@MnO_2 (290.0 μg/mL) under different pH values (5.0, 7.0 and 12.0) with H_2O_2.

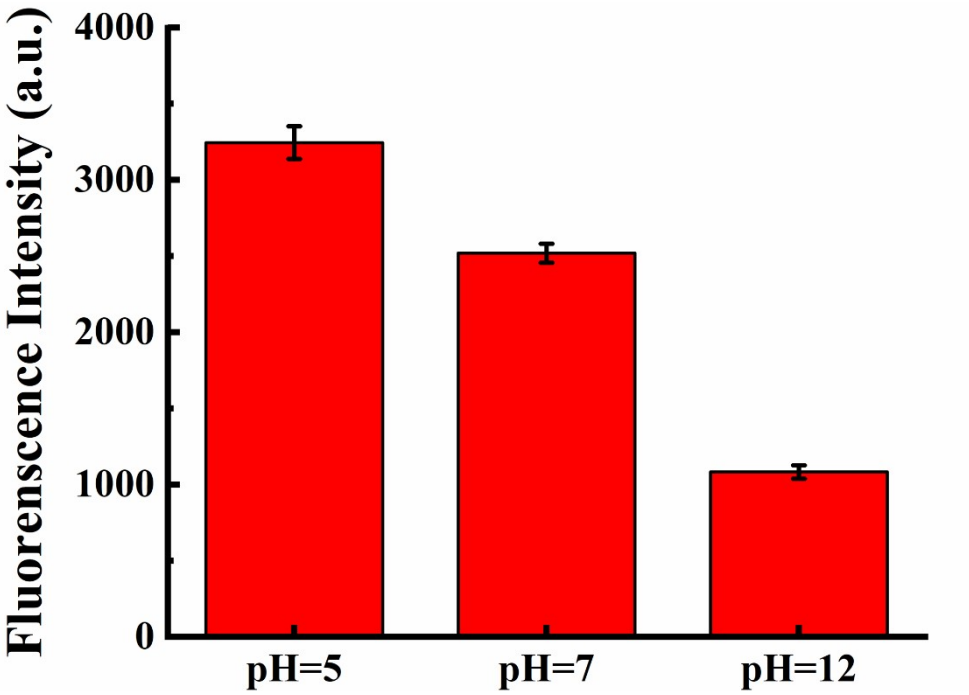

Figure S8. The PBS buffer solutions (pH = 5.0, 100 mM) with 1.0 mM H_2O_2 under different pH values was prepared from Yongjiang River to explore the stability of ZGC@MnO_2 (290.0 μg/mL) in complex environments.

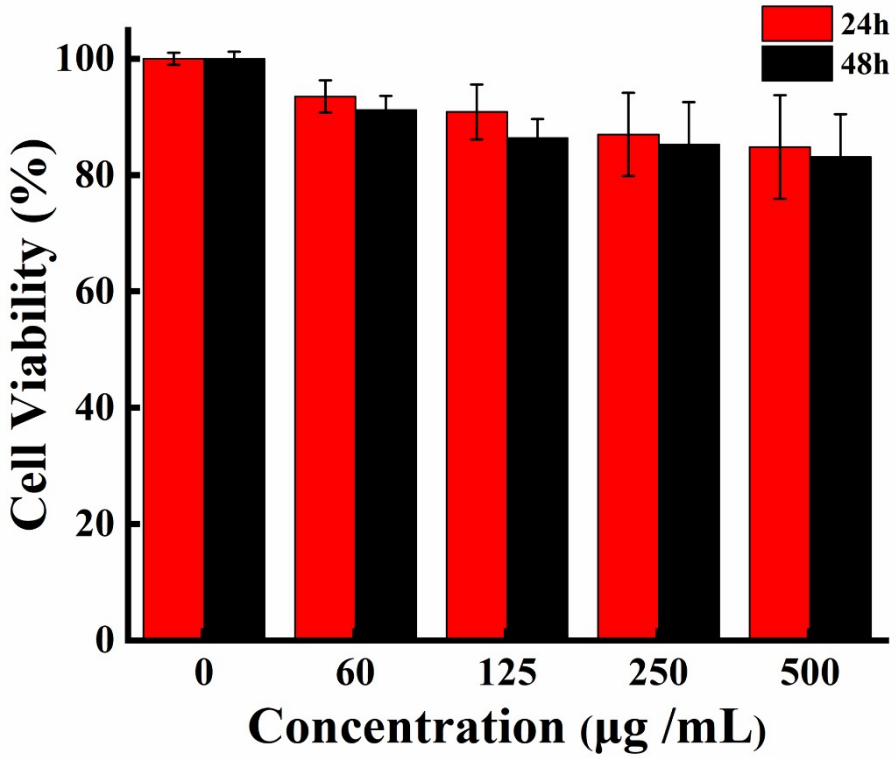

Figure S9. Cell viability of MCF-7 cells after being incubated with different concentrations of ZGC@MnO_2 for 24 h and 48 h.

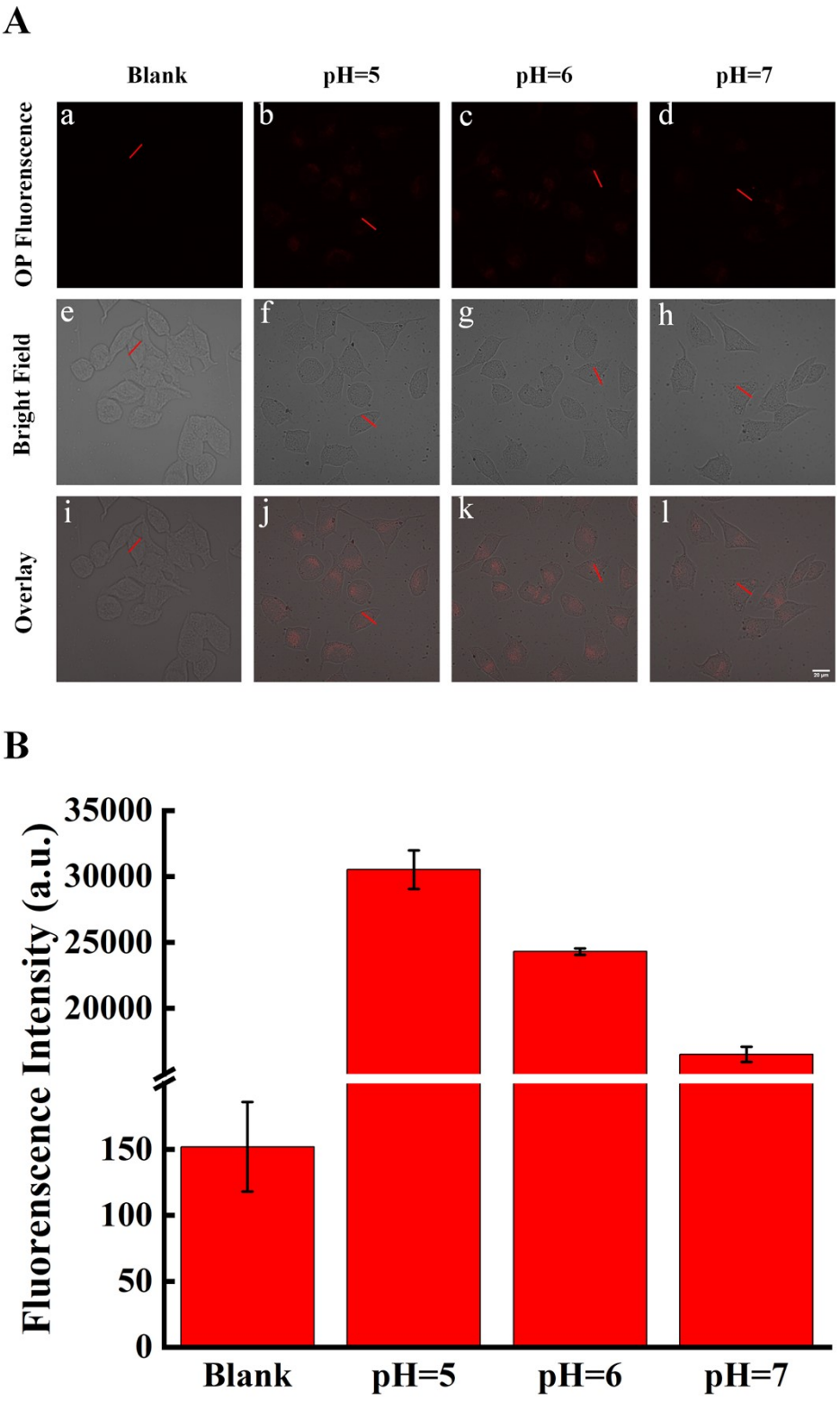

Figure S10. (A) The fluorescence response images of ZGC@MnO_2 (290.0 μg/mL) in cells under different pH conditions (pH=5, 6, 7). The scale bar is 20.0 μm. (B) The fluorescence intensity in cells of (A).

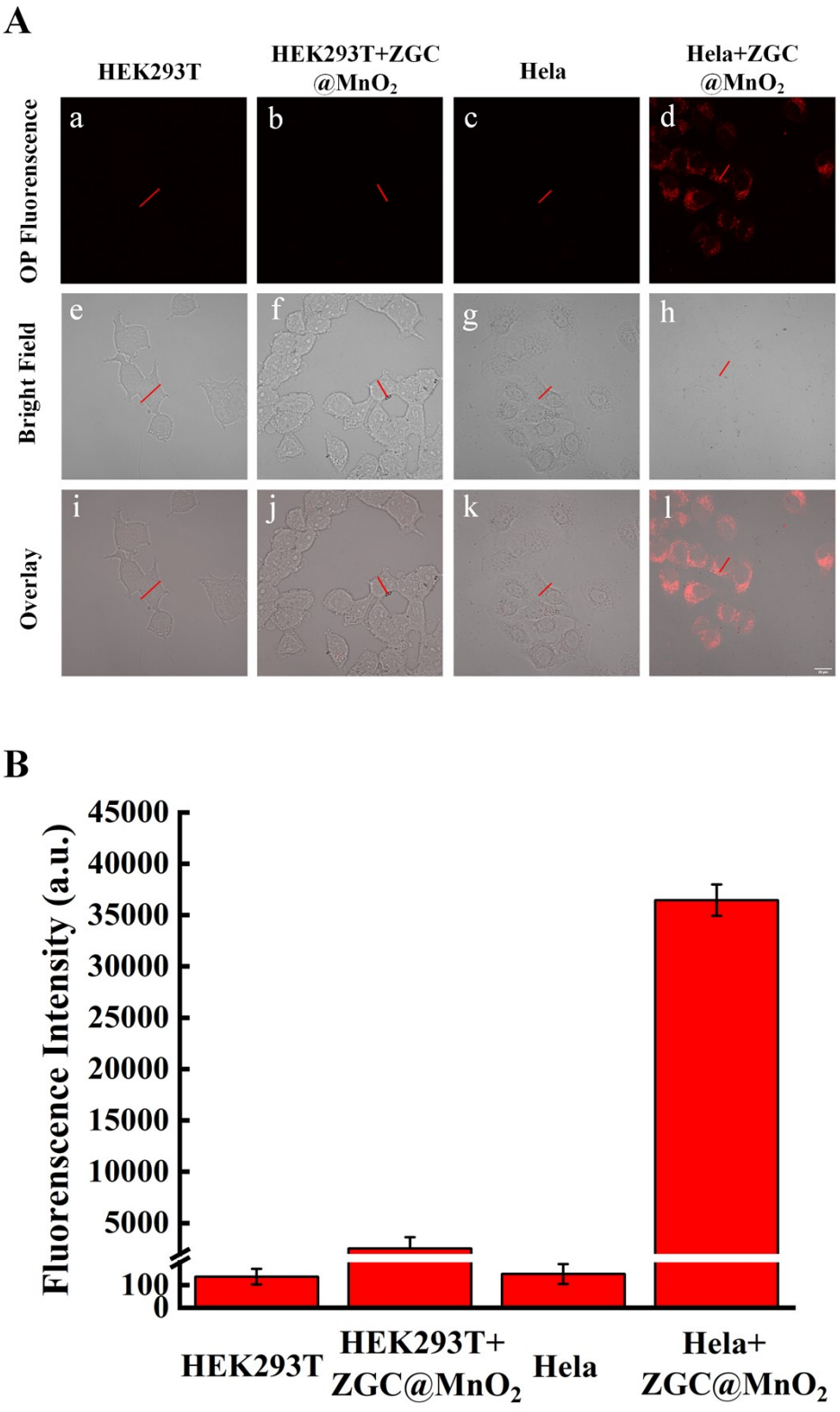

Figure S11. (A) The fluorescence images of ZGC@MnO_2 (HEPES, pH=5.0, 290.0 μg/mL) in normal cells (HEK293T, HEK293T+ZGC@MnO_2) and cancer cells (Hela, Hela+ZGC@MnO_2). The scale bar is 20.0 μm. (B) The fluorescence intensity in cells of (A).

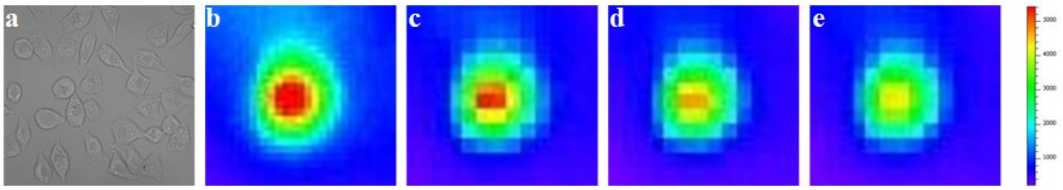

Figure S12. The ZGC@MnO_2 nanoprobe (290.0 μg/mL) in cells was irradiated with UV for 10 min followed by long afterglow imaging within 0-30min in IVIS (a: MCF-7 cells, b: 0.0 min, c: 10 min, d: 20 min, e: 30 min).

Table S1. Comparison of ZGC@MnO_2 with other nanoprobe

Nanoprobe	Advantages of the ZGC@MnO_2 compared with this nanoprobe	Reference
AuPd-PDA	AuPd-PDA nanotube-modified electrodes in the detection of H_2O_2. However, this probe relies on real-time electrochemical signals and cannot provide continuous signal output like long-persistence probes. Additionally, the preparation process involves the use of precious metals, which increases the production cost.	[1]
FeN_3/PtN_4	FeN_3/PtN_4 single atom nanozymes exhibit high sensitivity and rapid response in H_2O_2 detection. However, their complex preparation, susceptibility to interference from bioactive substances, and short signal duration compared to persistent luminescence probes limit their stability.	[2]
Si-CdTe QDs	Si-CdTe QDs probes exhibit high sensitivity and selectivity in H_2O_2 detection. However, ZGC@MnO_2 offers better detection accuracy and achieves detection through dual-mode imaging. Additionally, its luminescence signal in the near-infrared region is more suitable for deep-tissue imaging.	[3]
MTCN	Although MTCN achieves dual-mode H_2O_2 detection through fluorescence and photoacoustic imaging, ZGC@MnO_2 offers simpler preparation and it provides continuous signal output like long-persistence probes. The luminescence signal of ZGC@MnO_2 in the near-infrared region can reduce the interference of background signals in the organism.	[4]
TP-CQDs@MnO_2	Although this probe leverages two-photon advantages for deep tissue detection, ZGC@MnO_2 does not require *in-situ*	[5]

	excitation, and the luminescence signal of ZGC@MnO_2 in the near-infrared region can reduce the interference of background signals in the organism, making it more suitable for *in vivo* H_2O_2 detection.	

Table S2. Performance Comparison Between Developed Methods and Reported Methods

Method	Signal model	Resistance to background interference	Limit of detection (LOD)	Reference
AgNWs	Electrochemical	Medium	46 μM	[6]
$CuCo_2S_4$	Electrochemical	Low	0.084 mM	[7]
CD-NP-BE	Fluorescent (FRET-based)	High	0.5 μM	[8]
AuNPs/PEG	Electrochemical	High	170 nM	[9]
TMN-H_2O_2	Fluorescent (NIR-based)	High	76 nM	[10]
ZGC@MnO_2	Persistent luminescence and MR	High	3.67 nM	This work

5. References

1. G. L. He, F. L. Gao, W. Li, P. W. Li, X. F. Zhang, H. Yin, B. C. Yang, Y. B. Liu and S. R. Zhang, *Analytical Methods*, 2019, **11**, 1651-1656.
2. S. Wang, Z. F. Hu, Q. L. Wei, H. M. Zhang, W. N. Tang, Y. Q. Sun, H. Q. Duan, Z. C. Dai, Q. Y. Liu and X. W. Zheng, *Nano Research*, 2022, **15**, 4266-4273.
3. J. L. Zhou, R. X. Zhao, Y. Q. Du, S. K. Liu, W. T. Li, S. L. Gai, F. He, L. L. Feng and P. P. Yang, *Advanced Functional Materials*, 2022, **32**, 2112083.
4. T. Chen, Z. L. Chen, Q. T. Zhou, H. Y. Ding, P. Gong, J. Wang, H. L. Cai, R. J. Ao, M. L. Yu, J. B. Song, L. S. Lin and H. H. Yang, *Advanced Functional Materials*, 2022, **32**, 2208720.
5. H. Zhong, S. Yu, B. Li, K. He, D. Li, X. Wang and Y.-X. Wu, *Chemical Communications*, 2021, **57**, 6288-6291.

6. J. H. Lee, B.-C. Huynh-Nguyen, E. Ko, J. H. Kim and G. H. Seong, *Sensors and Actuators B: Chemical*, 2016, **224**, 789-797.
7. Z. Yang, S. Zhang, Y. Fu, X. Zheng and J. Zheng, *Electrochimica Acta*, 2017, **255**, 23-30.
8. G. Wu, F. Zeng, C. Yu, S. Wu and W. Li, *J Mater Chem B*, 2014, **2**, 8528-8537.
9. Z. Zhao and M. Zharnikov, *Nanomaterials (Basel)*, 2023, **13**, 3137.
10. G. Chunpo, Y. Yan, T. Pengfei, S. Hu, J. Yibo, S. Yuyang, Y. Yun and R. Feng, *Sensors and Actuators B: Chemical*, 2022, **350**, 130831.